Phase behavior of nanoparticle–copolymer films confined between polymer-grafted surfaces

2008 J. Phys.: Condens. Matter 20 095006

(http://iopscience.iop.org/0953-8984/20/9/095006)

J. Phys.: Condens. Matter **20** (2008) 095006 (5pp) doi:10.1088/0953-8984/20/9/095006

Phase behavior of nanoparticle–copolymer films confined between polymer-grafted surfaces

Ling Zhou and Yuqiang Ma

National Laboratory of Solid State Microstructures, Nanjing University, Nanjing 210093, People's Republic of China

E-mail: ZL7103@163.com

Received 1 November 2007, in final form 23 January 2008
Published 14 February 2008
Online at stacks.iop.org/JPhysCM/20/095006

Abstract

The self-assembly of nanoparticle–copolymer films confined between two polymer-grafted surfaces is studied by using self-consistent field and density functional theories. With increasing particle concentration, the film undergoes a series of transitions including hexagonal, lamellar, hexagonal-lamellar, double-core hexagonal and hexagonal-square structures. This behavior can be explained by the competition between the bulk phase behavior of the mixture, the wetting influence of polymer brushes and the steric packing effect of particles. The results provide an effective way to control the formation of stable highly-ordered microstructures within the film.

1. Introduction

Mixtures of nanoparticles and copolymers exist extensively in nature and much attention has been paid to their self-assembly, both theoretically and experimentally, in recent years [1–4]. The bulk phases of these kinds of mixtures display some self-assembled structures, such as the center-filled or edge-filled lamellar phase, hexagonally arranged cylinder phase and cylindrical phase in the matrix, which rely on the size of particles and the relative fraction of block components [5, 6]. Compared with the single-component system, these hybrid materials can significantly improve their mechanical, electronic or photonic properties, and therefore have many potential inspiring applications, especially in biomaterials, ceramics and semiconductors [7–9]. Further research on confined systems has indicated that the effects of environments on the self-assembly cannot be discounted [10–12]. Surface effects break the symmetry of the system, and the bulk phase behavior is restrained, while some other ordered structures are formed. We note that frustrated structures with islands or holes are often observed in confined copolymer films when the film thickness mismatches with the bulk phase [13]. At a suitable thickness, a lamellar phase can be formed in the mixtures of cubic particles and symmetric diblock copolymers confined between two solid surfaces. The orientation is either parallel or perpendicular to the confining solid surfaces, depending on the film thickness and the wetting properties of the confining surfaces [14, 15]. However, the phase behavior of the confined film of particles and asymmetric copolymers is still unclear. In this paper, we present a theoretical study of the self-assembly of a nanoparticle–asymmetric diblock copolymer thin film confined between two soft surfaces. The soft surfaces are modeled by polymer brushes. According to the earlier work by Ren and Ma [16, 17], entropic elasticity of polymer brushes can effectively control the shape of the interface and the thickness of the film to promote the existence of the bulk behavior in a confined system. To the best of our knowledge, there have been no systematic experimental or theoretical studies on the self-assembly of such a system. We try to seek an effective way to control the formation of difference microstructures in this film and avoid possible frustrated structures. Combined self-consistent field theory (SCFT) and density functional theory (DFT) developed by Balazs *et al* [5] are used. As is well known, SCFT for polymeric fluids successfully predicts the phase behavior of diblock copolymer melts, in good agreement with experiments [18, 19]. DFT is powerful in accounting for the steric packing effect of particles [20, 21]. The combination provides a reliable method for investigating the equilibrium morphologies and phase transitions of our system. In such system, many factors will influence the phase behavior, such as the length and the volume fraction of polymers, the size and the concentration of nanoparticles and the type and magnitude of interactions. We mainly

undertake a systematic study by varying the nanoparticle concentration and the density of grafting polymers. A phase diagram is constructed. As expected, except for the lamellar structure, a hexagonally arranged cylinder phase of the bulk phase is observed. Moreover, some new structures, such as double-core hexagons with different orientations and a hybrid structure of hexagons and squares, are obtained due to the cooperative behavior of particles and polymers which cannot be observed in a single-component system. The use of polymer brushes efficiently avoids the possible frustrated structures and promotes the formation of large-scale ordered structures. We expect that the present study may offer a mechanism for understanding the self-assembly behavior of confined nanoparticle–copolymer thin films.

2. Model details

We consider a mixture of nanoparticles and AB diblock copolymers confined between two parallel surfaces grafted by $n_{\rm br}$ B-type homopolymer chains. The surfaces are placed in the xy plane and located at $z = 0$ and $z = L_z$, respectively. Both homopolymer and copolymer chains consist of N segments of length a. The A-monomer fraction of copolymers is denoted by f. We assume that each segment occupies a fixed volume ρ_0^{-1}, and that the system is incompressible with a total volume V. Because of the translational invariance along the y axis, the calculation can be reduced to the xz plane. Then the volume V can be written as $L_x \times L_z$, where L_x is the lateral length of the surface along the x axis. The grafting density of brushes is defined as $\sigma = n_{\rm br}/2L_x$, and the average volume fraction is $\phi_{\rm br} = n_{\rm br}N\rho_0^{-1}/V$. By introducing the particle concentration $\psi_{\rm p}$ of the mixture, the average volume fraction of particles is expressed as $\phi_{\rm p} = (1-\phi_{\rm br})\psi_{\rm p}$, and that of the copolymers is $\phi_{\rm co} = 1-\phi_{\rm br}-\phi_{\rm p}$.

In the framework of the SCF/DFT approach, the free energy F for the present system is given by:

$$\begin{aligned}\frac{NF}{\rho_0 k_{\rm B}TV} &= -\phi_{\rm br}\ln\left(\frac{Q_{\rm br}}{V\phi_{\rm br}}\right) - \phi_{\rm co}\ln\left(\frac{Q_{\rm co}}{V\phi_{\rm co}}\right)\\ &- \frac{\phi_{\rm p}}{\alpha_{\rm p}}\ln\left(\frac{Q_{\rm p}\alpha_{\rm p}}{V\phi_{\rm p}}\right) + \frac{1}{V}\int {\rm d}\mathbf{r}[\chi_{\rm ab}N\varphi_{\rm a}(\mathbf{r})\varphi_{\rm b}(\mathbf{r})\\ &+ \chi_{\rm abr}N\varphi_{\rm a}(\mathbf{r})\varphi_{\rm br}(\mathbf{r}) + \chi_{\rm bbr}N\varphi_{\rm b}(\mathbf{r})\varphi_{\rm br}(\mathbf{r})\\ &+ \chi_{\rm ap}N\varphi_{\rm a}(\mathbf{r})\varphi_{\rm p}(\mathbf{r}) + \chi_{\rm bp}N\varphi_{\rm b}(\mathbf{r})\varphi_{\rm p}(\mathbf{r})\\ &+ \chi_{\rm brp}N\varphi_{\rm br}(\mathbf{r})\varphi_{\rm p}(\mathbf{r}) - W_{\rm a}(\mathbf{r})\varphi_{\rm a}(\mathbf{r}) - W_{\rm b}(\mathbf{r})\varphi_{\rm b}(\mathbf{r})\\ &- W_{\rm br}(\mathbf{r})\varphi_{\rm br}(\mathbf{r}) - W_p(\mathbf{r})\rho_{\rm p}(\mathbf{r}) - \xi(\mathbf{r})(1-\varphi_{\rm a}(\mathbf{r})\\ &- \varphi_{\rm b}(\mathbf{r}) - \varphi_{\rm br}(\mathbf{r}) - \varphi_{\rm p}(\mathbf{r})) + \rho_{\rm p}\Psi(\bar{\varphi}_{\rm p})], \end{aligned} \tag{1}$$

where $k_{\rm B}$ is the Boltzmann constant and T is the temperature. $\varphi_{\rm br}(\mathbf{r})$, $\varphi_{\rm a}(\mathbf{r})$, $\varphi_{\rm b}(\mathbf{r})$ and $\varphi_{\rm p}(\mathbf{r})$ are the local volume fractions of brushes, A blocks, B blocks, and particles, respectively. $\xi(\mathbf{r})$ is a Lagrange-multiplier field invoked by the incompressibility of the system. $\chi_{ij}(i, j = {\rm br, a, b, p})$ characterizes the interaction between species i and j. $Q_{\rm br} = \int {\rm d}\mathbf{r}\, q_1(\mathbf{r}, s)q_1^+(\mathbf{r}, s)$ and $Q_{\rm co} = \int {\rm d}\mathbf{r}\, q_2(\mathbf{r}, s)q_2^+(\mathbf{r}, s)$ are single-chain partition functions of brushes and copolymers in the effective chemical potential fields $W_{\rm br}(\mathbf{r})$, $W_{\rm a}(\mathbf{r})$, $W_{\rm b}(\mathbf{r})$, respectively. Similarly, $Q_{\rm p} = \int {\rm d}\mathbf{r}\exp[-W_{\rm p}(\mathbf{r})]$ is the partition function of particles under the effective chemical potential field $W_{\rm p}(\mathbf{r})$. $q_i(\mathbf{r}, s)$ and $q_i^+(\mathbf{r}, s)(i = 1, 2)$ are the propagators representing the probabilities of finding segment s at position $\mathbf{r}$ from two distinct ends of chains, which satisfy the modified diffusion equations $\partial q_i/\partial s = (a^2N/6)\,\nabla^2 q_i - W_i(\mathbf{r})q_i$ and $\partial q_i^+/\partial s = -(a^2N/6)\,\nabla^2 q_i^+ + W_i(\mathbf{r})q_i^+$. The initial condition for brushes is $q_1(x, z = 0 \text{ or } L_z, 0) = 1$, $q_1(x, z \neq 0 \text{ or } L_z, 0) = 0$, and $q_1^+(x, z, 1) = 1$, and that for copolymers is $q_2(x, z, 0) = 1$ and $q_2^+(x, z, 1) = 1$. $\alpha_{\rm p}$ is the volume ratio of the nanoparticles to polymer chains given by $\alpha_{\rm P} = v_R/N\rho_0^{-1}$, where $v_R = (4/3)\pi R^3$ is the volume of the nanoparticles with radius R. $\rho_{\rm p}$ is the particle center distribution, and the corresponding local particle volume fraction is given by

$$\varphi_{\rm p}(\mathbf{r}) = (\alpha_{\rm p}/v_R)\int_{|\mathbf{r}'|<R} {\rm d}\mathbf{r}'\rho_{\rm p}(\mathbf{r}+\mathbf{r}'). \tag{2}$$

The steric packing effect of nanoparticles is included in the last term on the right-hand side of equation (1). $\Psi(\bar{\varphi}_{\rm p})$ can be calculated by using the Carnahan–Starling formula [22], $\Psi(x) = (4x - 3x^2)/(1-x)^2$, where the weighted particle density $\bar{\varphi}_{\rm p}(\mathbf{r})$ is given by $\bar{\varphi}_{\rm p}(\mathbf{r}) = (\alpha/v_{2R})\int_{|\mathbf{r}'|<2R} {\rm d}\mathbf{r}'\rho_{\rm p}(\mathbf{r}+\mathbf{r}')$. v_{2R} is the volume of a sphere with radius $2R$ around $\mathbf{r}$.

Minimizing the free energy in equation (1), with respect to $W_{\rm a}$, $W_{\rm b}$, $W_{\rm br}$, W_p, $\varphi_{\rm a}$, $\varphi_{\rm b}$, $\varphi_{\rm br}$, $\varphi_{\rm p}$, and ξ, leads to the following self-consistent equations at the equilibrium:

$$\varphi_{\rm a}(\mathbf{r}) = \frac{\phi_{\rm co}V}{Q_{\rm co}}\int_0^f {\rm d}s q_2(\mathbf{r}, s)q_2^+(\mathbf{r}, s) \tag{3}$$

$$\varphi_{\rm b}(\mathbf{r}) = \frac{\phi_{\rm co}V}{Q_{\rm co}}\int_f^1 {\rm d}s q_2(\mathbf{r}, s)q_2^+(\mathbf{r}, s) \tag{4}$$

$$\varphi_{\rm br}(\mathbf{r}) = \frac{\phi_{\rm br}V}{Q_{\rm br}}\int_0^1 {\rm d}s q_1(\mathbf{r}, s)q_1^+(\mathbf{r}, s) \tag{5}$$

$$\rho_{\rm p}(\mathbf{r}) = \frac{\phi_{\rm p}V}{\alpha_{\rm p}Q_p}\exp[-W_{\rm p}(\mathbf{r})] \tag{6}$$

$$W_{\rm a}(\mathbf{r}) = \chi_{\rm ab}N\varphi_{\rm b}(\mathbf{r}) + \chi_{\rm abr}N\varphi_{\rm br}(\mathbf{r}) + \chi_{\rm ap}N\varphi_{\rm p}(\mathbf{r}) + \xi(\mathbf{r}) \tag{7}$$

$$W_{\rm b}(\mathbf{r}) = \chi_{\rm ab}N\varphi_{\rm a}(\mathbf{r}) + \chi_{\rm bbr}N\varphi_{\rm br}(\mathbf{r}) + \chi_{\rm bp}N\varphi_{\rm p}(\mathbf{r}) + \xi(\mathbf{r}) \tag{8}$$

$$W_{\rm br}(\mathbf{r}) = \chi_{\rm abr}N\varphi_{\rm a}(\mathbf{r}) + \chi_{\rm bbr}N\varphi_{\rm b}(\mathbf{r}) + \chi_{\rm brp}N\varphi_{\rm p}(\mathbf{r}) + \xi(\mathbf{r}) \tag{9}$$

$$\begin{aligned}W_{\rm p}(\mathbf{r}) &= \Psi(\bar{\varphi}_{\rm p}(\mathbf{r})) + \frac{\alpha_{\rm p}}{v_R}\int_{|\mathbf{r}'|<R} {\rm d}\mathbf{r}'[\chi_{\rm ap}N\varphi_{\rm a}(\mathbf{r}+\mathbf{r}')\\ &+ \chi_{\rm bp}N\varphi_{\rm b}(\mathbf{r}+\mathbf{r}') + \chi_{\rm brp}N\varphi_{\rm br}(\mathbf{r}+\mathbf{r}') + \xi(\mathbf{r}+\mathbf{r}')]\\ &+ \frac{\alpha_{\rm p}}{v_{2R}}\int_{|\mathbf{r}'|<2R} d\mathbf{r}'[\rho_{\rm p}(\mathbf{r}+\mathbf{r}')\Psi'(\bar{\varphi}_{\rm p}(\mathbf{r}+\mathbf{r}'))] \end{aligned} \tag{10}$$

$$\varphi_{\rm a}(\mathbf{r}) + \varphi_{\rm b}(\mathbf{r}) + \varphi_{\rm br}(\mathbf{r}) + \varphi_{\rm p}(\mathbf{r}) = 1. \tag{11}$$

The calculation starts from the initial random fields $W_i(\mathbf{r})$ $(i = {\rm a, b, br, p})$. The diffusion equations are then solved to obtain $q_i(\mathbf{r}, s)$ and $q_i^+(\mathbf{r}, s)$ $(i = 1, 2)$ by using a Frank–Nicholson scheme and an alternating-direct implicit (ADI) method. Next, volume fractions are evaluated by equations (2)–(6), and the new fields can be obtained from equations (7)–(10) by the substitution of the volume fractions. The iteration repeats until the free energy difference between two iterations is smaller than 10^{-6} and the incompressible condition is satisfied. In calculations, the simulations are repeated 10–20 times using different initial random fields at each particle concentration. Free energies of different structures are compared to search for the stable state with the lowest free energy. All the sizes are in units of a.

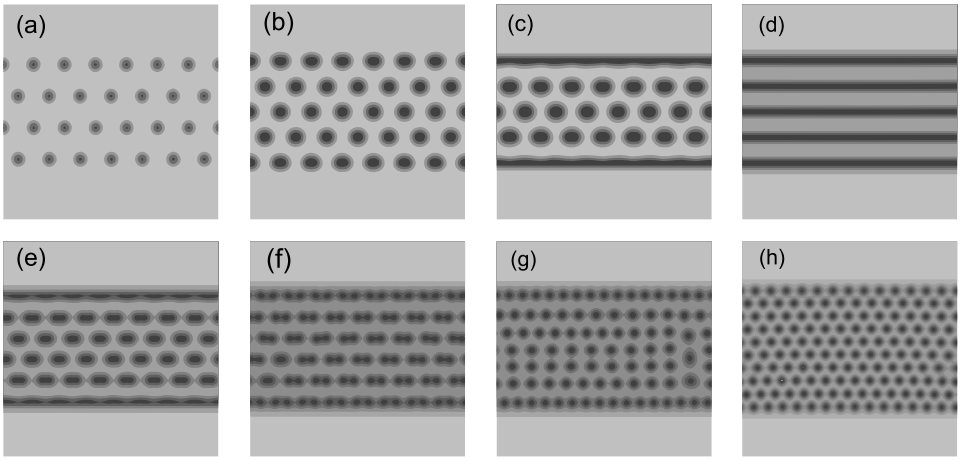

Figure 1. Density distributions of particles at a fixed grafting density $\sigma = 0.2$ with an increase in the particle concentration ψ_p: (a) $\psi_p = 0.05$, (b) $\psi_p = 0.125$, (c) $\psi_p = 0.16$, (d) $\psi_p = 0.2$, (e) $\psi_p = 0.225$, (f) $\psi_p = 0.25$, (g) $\psi_p = 0.26$, (h) $\psi_p = 0.295$.

3. Results and discussion

In the present simulations we focus on the effects of the particle concentration and the grafting density on the phase behavior of the film. Our parameters are then reduced to two: ψ_p and σ. Other parameters are set as $N = 100$, $L_x = L_z = 100a$, $f = 0.2$. The particle radius R is taken to be $0.2r_0$, where $r_0 = aN^{1/2}$ is the natural size of free polymers. The periodic boundary condition is applied in the x direction, and the regions of $z < 1$ and $z > L_z$ are forbidden. Further, we assume that the nanoparticles preferentially wet to the A blocks. The Flory interaction parameters are chosen as $\chi_{ab}N = \chi_{abr}N = \chi_{bp}N = \chi_{brp}N = 20$, $\chi_{ap}N = \chi_{bbr}N = 0$.

We first discuss the equilibrium morphologies of the film. Figure 1 shows the density distributions of particles at six typical particle concentrations ($\psi_p = 0.05, 0.125, 0.16, 0.2, 0.25, 0.295$) with a fixed grafting density $\sigma = 0.2$. With an increase in particle concentration ψ_p, the film assembles into sparse hexagonal, dense hexagonal, hexagonal-lamellar, lamellar, hexagonal-lamellar, double-core hexagonal, hexagonal-square and denser hexagonal structures in turn. In the absence of the confining surfaces, the bulk phase of the mixture is always a hexagonally arranged cylinder structure. However, the polymer brushes are strongly stretched and prefer to form a flat interface. These two factors compete with each other in the confined film and result in the formation of the final structures. In other words, this ordering mechanism can be explained by the interplay of interface energy, entropy and steric packing effect of particles. When $\psi_p = 0.05$, the interface energy between the A and B blocks is dominant, which leads to the formation of the four-layered hexagonal phase. The compatibility of the particles with the A blocks makes the particles distribute into the domains of the A blocks and form a hexagonal structure. When $\psi_p = 0.125$, the further increased total interface energy benefited from the increasing particle–B block interface energy leading to the formation of a five-layered hexagonal structure. However, this structure cannot be retained if we further increase the concentration of particles. When $\psi_p = 0.2$, a lamellar structure is observed. In this case, the wetting effect of brush-formed surface to the B blocks plays a more important role. If the particle concentration is somewhat lower or higher than the values that form the lamellar structure such as $\psi_p = 0.16$ and 0.225, a hexagonal-lamellar mixed phase will emerge. In the region that is close to the brush surface, the film tends to form lamellae, while it still keeps a hexagonal structure in the middle of the region. However, we find that figure 1(e) is slightly different from figure 1(c). Obviously, a denser structure is formed. Moreover, the particle distribution begins to slightly orient along the surface. With the increasing particle concentration, the effect of particles becomes more and more important. As we see, the thin film shows a very interesting structure at $\psi_p = 0.25$ which cannot be observed in the single-component system [16]. We call it the 'double-core' hexagonal structure (see figure 1(f)). The particle distribution shows two peak values at each lattice point of the hexagonal structure and the orientation is parallel to the surfaces. The powerful interface energy favors driving the mixture to form a dense hexagonal structure. On the other hand, the quickly increased steric packing energy prefers to push the particles apart. The equilibrium of such energies finally determines this more complicated phase structure. With the further addition of the particles, the steric packing effect will be dominant. The double core continues to split and a seven-layered hexagonal and square mixed structure is formed when $\psi_p = 0.26$. However, this structure only exists in a very narrow concentration range. When $\psi_p = 0.295$, a 10-layered denser hexagonal structure may be observed. These large arrays of the microstructure have potentials to be used in semiconductors with excellent electronic properties [7].

Further we examine the role of the polymer brushes in the self-assembly process. Figure 2 gives the density profiles of the polymer brushes at four typical particle concentrations $\psi_p = 0.05, 0.125, 0.2$ and 0.295. Figures 2(a), (b) and (d) illustrate curved interfaces corresponding to the hexagonal structures, and figure 2(c) displays a flat interface corresponding to the lamellar structure. As mentioned earlier, the existence of the polymer brushes effectively avoids the

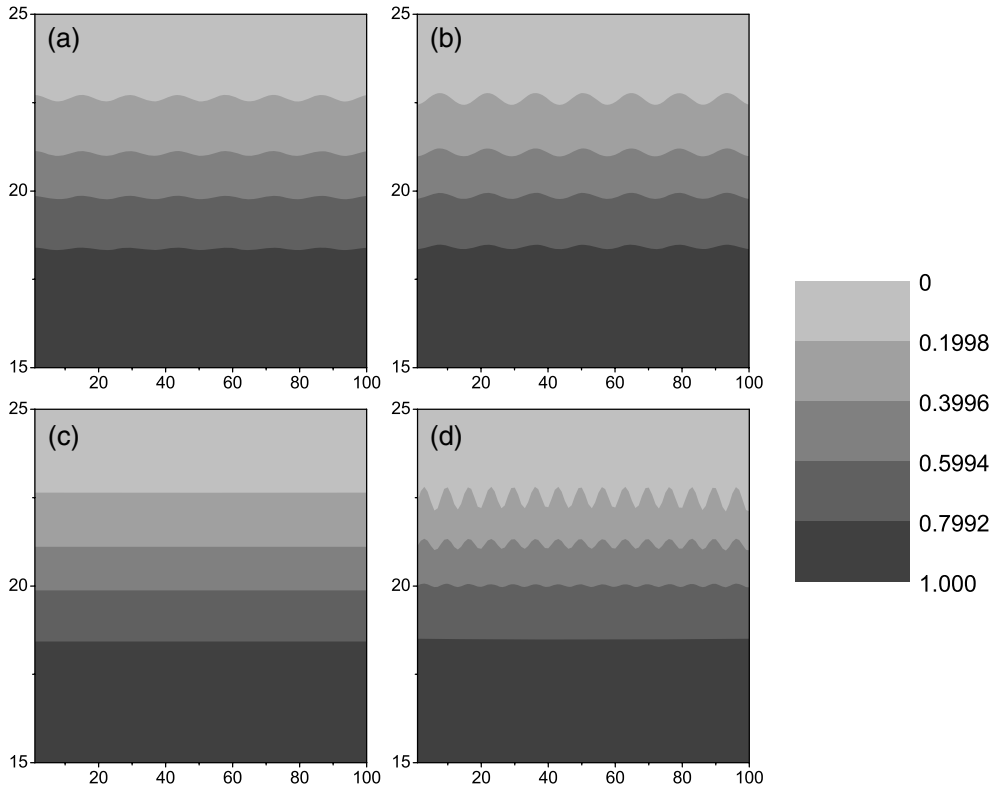

Figure 2. Density profiles of polymer brushes with (a) $\psi_p = 0.05$, (b) $\psi_p = 0.125$, (c) $\psi_p = 0.2$ and (d) $\psi_p = 0.295$.

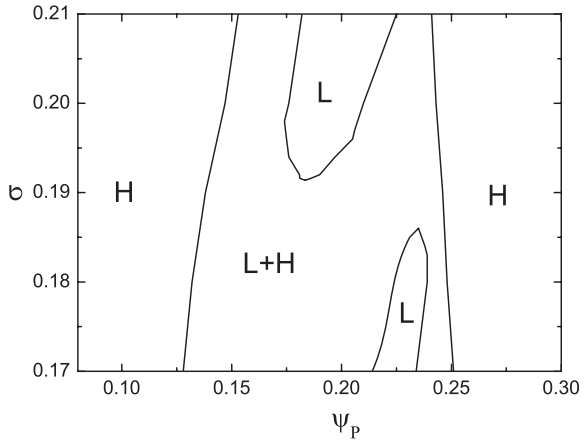

Figure 3. Phase diagram as a function of the grafting density σ and the particle concentration ψ_p: H, hexagonal structure; L, lamellar structure; L + H, hexagonal-lamellar mixed structure.

possible frustration caused by the incompatibility between the different microstructures and the film thickness. Though the brush density close to the confining surfaces remains unchanged at a given grafting density, the other end of the brushes can deform to construct a flat or rugate interface to match the formation of different microstructures required by the minimization of the total free energy.

Finally, to provide useful information about the structural changes of the system, we calculate the phase diagram in the plane of the grafting density and the particle concentration, as shown in figure 3. We find that the phase boundary becomes very difficult to distinguish at high particle concentrations. Sometimes different-layered or single- and double-core hexagonal mixed structures are observed. More interesting, there exist two kinds of double-core hexagonal structures oriented vertically to each other when $\sigma = 0.21$. The orientation is vertical to the confining surfaces at $\psi_p = 0.23$ (see figure 4(a)) and switches to be parallel to the surfaces at $\psi_p = 0.246$ (see figure 4(b)). For clarity, we only give the phase boundary of hexagonal, lamellar and hexagonal-lamellar structures. Different-layered hexagonal states, the hexagonal-square state and other hexagonal mixed structures are all contained in the hexagonal phase region. The chosen grafting density changes from 0.17 to 0.21, which ensures both the entropic effects of the brushes and the effective film thickness. We find that at any given grafting density, hexagonal and hexagonal-lamellar structures always exist. However, if we give the grafting density in the range of 0.186–0.1914, pure lamellar structures cannot be formed. When $\sigma \leqslant 0.186$, lamellar structures have six layers but change to five layers when $\sigma \geqslant 0.1914$. The appearance of the hexagonal-lamellar structures can be explained by the mismatch of the film thickness with the period of the lamellar structure when $0.186 < \sigma < 0.1914$. In this case, the change of the interface energy and entropy caused by brushes cannot compensate for the enthalpy of the mixture, so only the hexagonal-lamellar mixed structure is observed. Further, we note that with the increase of ψ_p, the system experiences a hexagonal reentrant transition at a fixed grafting density. Similarly, when $0.214 < \psi_p < 0.225$, the system shows a lamellar $\longrightarrow$ hexagonal-

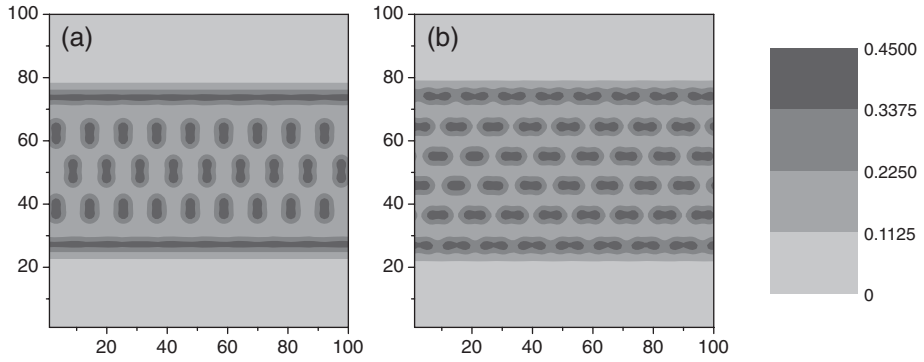

Figure 4. Density distributions of particles at the grafting density $\sigma = 0.21$. (a) $\psi_p = 0.23$, (b) $\psi_p = 0.246$.

lamellar ⟶ lamellar reentrant transition with varying grafting density.

4. Conclusions

We have presented the phase behavior of a particle–copolymer thin film confined between two polymer-grafted surfaces. With the increase of the particle concentration, the film assembles into sparse hexagonal, dense hexagonal, hexagonal-lamellar, lamellar, hexagonal-lamellar, double-core hexagonal, hexagonal-square and more dense hexagonal structures. We conclude that at lower particle concentrations, the formation of the hexagonal structure is mainly attributed to the interfacial tension between the A and B blocks. At intermediate concentrations, the appearance of the lamellar structure mainly generates from the wetting effects of the brush-formed interface at a suitable film thickness. At higher particle concentrations, the interface energy between nanoparticles and the B blocks and the excluded-volume effect of the particles are dominant, and promote the formation of the more complicated structures. The introduced soft interfaces not only effectively avoid the possible frustrated phase, but also promote the formation of the new structures. Furthermore, we give a phase diagram as a function of the grafting density and the particle concentration, which shows two kinds of reentrant structure transitions. One is the hexagonal reentrant transition changing from left to right in the phase diagram at any fixed grafting density, and the other is the lamellar reentrant transition from bottom to top at a suitable particle concentration. In the process of self-assembly, the emergence of 'double-core' hexagonal structure is a very interesting result, which cannot be observed in the confined single-component system. The change of the orientation in figure 4 can be used to create a switching effect. And the large arrays of the microstructure may provide a helpful guidance to fabricate the functionally useful materials. The results provide an effective way to control the formation of different highly-ordered microstructures within the films.

Acknowledgments

This work was supported by the National Basic Research Program of China, no. 2007CB925101, and the National Natural Science Foundation of China, nos 20490220, 20674037 and 10574061.

References

[1] Templin M, Franck A, DuChesne A, Leist H, Zhang Y M, Ulrich R, Schadler V and Wiesner U 1997 *Science* **278** 1795
[2] Zhao D, Feng J, Huo Q, Melosh N, Fredrickson G H, Chmelka B F and Stucky G D 1998 *Science* **279** 548
[3] Balazs A C 2000 *Curr. Opin. Colloid Interface Sci.* **4** 443
[4] de Hoog E H A, Kegel W K, van Blaaderen A and Lekkerkerker H N W 2001 *Phys. Rev.* E **64** 021407
[5] Thompson R B, Ginzburg V V, Matsen M W and Balazs A C 2001 *Science* **292** 2469
[6] Thompson R B, Ginzburg V V, Matsen M W and Balazs A C 2002 *Macromolecules* **35** 1060
[7] Stupp S I and Braun P V 1997 *Science* **277** 1242
[8] Kresge C T, Leonowicz M E, Roth W J, Vartuli J C and Beck J S 1992 *Nature* **359** 710
[9] Berman A, Addadi L and Weiner S 1988 *Nature* **331** 546
[10] Matsen M W 1997 *J. Chem. Phys.* **106** 7781
[11] Petera D and Muthukumar M 1998 *J. Chem. Phys.* **109** 5101
[12] Geisinger T, Muller M and Binder K 1999 *J. Chem. Phys.* **111** 5241
[13] Ren C L, Chen K and Ma Y Q 2005 *J. Chem. Phys.* **122** 154904
[14] Lee J Y, Shou Z and Balazs A C 2003 *Phys. Rev. Lett.* **91** 136103
[15] Lee J Y, Shou Z and Balazs A C 2003 *Macromolecules* **36** 7730
[16] Ren C L and Ma Y Q 2006 *J. Am. Chem. Soc.* **128** 2733
[17] Ren C L and Ma Y Q 2005 *Phys. Rev.* E **72** 051804
[18] Matsen M W and Schick M 1994 *Phys. Rev. Lett.* **72** 2660
[19] Matsen M W 1995 *Macromolecules* **28** 5765
[20] Tarazona P and Evans R 1984 *Mol. Phys.* **52** 847
[21] Tarazona P 1984 *Mol. Phys.* **52** 81
[22] Carnahan N F and Starling K E 1969 *J. Chem. Phys.* **51** 635